

Entropy of He II from 1.6 K to the  $\lambda$  line

Alan Singaas and Guenter Ahlers

*Department of Physics, University of California, Santa Barbara, California 93106*

(Received 18 November 1983)

The fountain pressure of He II was measured and the results were used to obtain the entropy from 1.6 K to near  $T_\lambda$  at vapor pressure and from 1.7 K to near  $T_\lambda$  at various pressures up to 29 bar. The data have a precision of  $\pm 0.1\%$  and an accuracy of  $\pm 0.5\%$ . There is excellent agreement with recent calorimetric measurements at vapor pressure and good agreement within the combined error estimates with some, but not all, previous fountain-pressure measurements. The small quantity  $\Delta S = \int_{T_0}^{T_\lambda} (C_p/T) dT$  was added to our measurements near  $T_\lambda$  to yield values for  $S_\lambda(P)$  which were fitted to an empirical equation with a scatter of  $\pm 0.1\%$ . The increased accuracy of our new measurements will reduce considerably the experimental errors in the determination of the superfluid fraction from the second-sound velocity near the superfluid transition line.

## I. INTRODUCTION

There has been much interest in recent years<sup>1</sup> in making high-precision measurements near the superfluid transition of liquid  $^4\text{He}$  in order to test the predictions of the renormalization-group theory of critical phenomena.<sup>2</sup> The entropy of He II is one of several experimentally accessible quantities that are related to critical properties of the  $\lambda$  transition through the predictions of two-fluid hydrodynamics.<sup>3,4</sup> In particular, the entropy per unit mass,  $S$ , is a necessary parameter in deriving the superfluid fraction  $\rho_s/\rho$  from measurements of the second-sound velocity  $u_2$  in He II.<sup>4</sup> For this reason, it is desirable to know  $S$  to a high degree of accuracy.<sup>5</sup>

The entropy of liquid helium can, of course, be obtained in the usual way from the specific heat  $C$  by integrating  $C/T$ . For the superfluid phase of  $^4\text{He}$ , it is also possible to derive the entropy from measurements of the first-, second-, and fourth-sound velocities or by measuring the fountain pressure (FP). In this paper we report entropy measurements using the FP method.

London<sup>6</sup> and Landau<sup>3</sup> have shown that, for a sample of He II contained in two volumes connected by a superleak, a small temperature difference  $\delta T$  between the volumes will result in a FP given by

$$\delta P = \rho S \delta T, \quad (1)$$

where  $\rho$  is the density of the liquid. The effect was first observed by Allen and Jones;<sup>7</sup> early measurements of the FP at vapor pressure were those of Meyer and Mellink,<sup>8</sup> with an accuracy of 10%, and Brewer and Edwards,<sup>9</sup> with an accuracy of 5%. van den Meijdenberg *et al.*<sup>10</sup> made extensive measurements from 1.15 K to near  $T_\lambda$  at pressures from saturated vapor pressure (SVP) to 25 bar. Their stated accuracy is about 3%, but the use of a room-temperature manometer required making corrections, the accuracy of which is difficult to evaluate. Sudraud and Varoquaux<sup>11</sup> measured the FP at various pressures from 1 to 25 bar and at temperatures between 0.7 K and  $T_\lambda$ ; however, above 1.35 K their measurements were taken at

pressures of 1 and 24 bar only. They state their accuracy as  $\pm 1\%$  with a "maximum error" of  $\pm 3\%$ .

In addition to the FP measurements listed above, there is a good deal of information about the entropy based on calorimetric and ultrasonic experiments. Lounasmaa and co-worker<sup>12,13</sup> measured the specific heat below  $T_\lambda$  at SVP and used their results to calculate the entropy with an accuracy of  $\pm 3\%$ . Ahlers<sup>14</sup> used their  $\lambda$ -point value as the integration constant in calculating  $S_\lambda$  at higher pressures by integrating  $(\partial S/\partial T)_\lambda$  derived from measurements of  $C_v$  and  $(\partial P/\partial T)_v$ . The resulting values along the  $\lambda$  line agree within 1% or 2% with calorimetric results under pressure by Lounasmaa.<sup>13</sup> Greywall and Ahlers,<sup>15</sup> in the analysis of their second-sound velocity measurements, used the  $S_\lambda$  obtained in this way, together with the integrated specific heat at constant pressure from Ref. 14, to obtain the entropy along isobars in the range  $T_\lambda - T \leq 0.1$  K at SVP and  $T_\lambda - T \leq 0.02$  K at higher pressures. The uncertainty in the entropy near  $T_\lambda(P)$  obtained in this manner is largely due to the uncertainty in  $S_\lambda$  and was the motivation for the present work. Maynard<sup>16</sup> used the values of  $S_\lambda$  from Ref. 14 mentioned above, an average of calorimetric data at 1.2 K and SVP,<sup>17</sup> and the high-precision measurements of first, second, and fourth sound by Heiserman *et al.*<sup>18</sup> to calculate values of the entropy from 1.2 K to near  $T_\lambda$  at pressures from 0 to 25 bar. Aside from his uncertainty in the value at 1.2 K and SVP, he states that his precision is no worse than  $\pm 0.6\%$  at the highest temperatures. Of course, his results close to  $T_\lambda$  depend heavily on the asymptotic values of  $S_\lambda$  from Ref. 14 that were built into his fitting equations. Finally, a preliminary analysis of heat-capacity measurements by Hoffer and Phillips<sup>19</sup> has yielded entropy values at SVP from very low temperatures to  $T_\lambda$ . Their result for  $S_\lambda$  is about 1.4% higher than that of Lounasmaa and co-worker.<sup>12,13</sup>

From the investigations discussed in the previous paragraphs, we know the entropy in the vicinity of the  $\lambda$  line with an absolute accuracy of perhaps  $\pm 2\%$  or  $\pm 3\%$  (leading to an absolute accuracy for  $\rho_s/\rho$  derived<sup>15</sup> from  $u_2$  of

5–8%). More accurate data are highly desirable, especially to help settle the important issue of possible departures from two-scale-factor universality along the  $\lambda$  line, which is discussed in detail in Ref. 1. We therefore measured the FP over the temperature range from 1.6 K to  $T_\lambda$  at pressures from SVP to 29 bar with a precision of  $\pm 0.1\%$  and an absolute accuracy of  $\pm 0.5\%$ . A new analysis of the second-sound velocity, using the new entropy data, will be presented elsewhere.<sup>20</sup>

In Sec. II of this paper we describe the experimental apparatus, the calibration procedures used for the thermometers and pressure gauges, and the measurement techniques used to obtain the FP. This section also contains an analysis of the possible experimental errors in our measurements. Section III contains the tabulated values of the measured FP entropies and a comparison of the entropy per mole derived from these results to previous measurements by other authors. In Sec. IV we summarize the results.

## II. EXPERIMENT

### A. General cryogenic apparatus

The main features of the cryogenic apparatus<sup>21</sup> are shown in Fig. 1. The entire assembly is contained in a stainless-steel vacuum can surrounded by a liquid-helium bath which can be kept at 4.2 K or pumped to 1.3 K. The first level inside the can is a continuous  $^4\text{He}$  refrigerator<sup>22</sup> with a volume of about 5 cm<sup>3</sup>. The operating temperature of the refrigerator was about 1.4 K, stable to about 2 mK. Below this level is an isothermal platform<sup>23</sup> which was regulated at a temperature between 1.5 and 1.8 K with a stability of about 10  $\mu\text{K}$ . This stage contains two hydraulically operated valves,<sup>24</sup> only one of which is shown

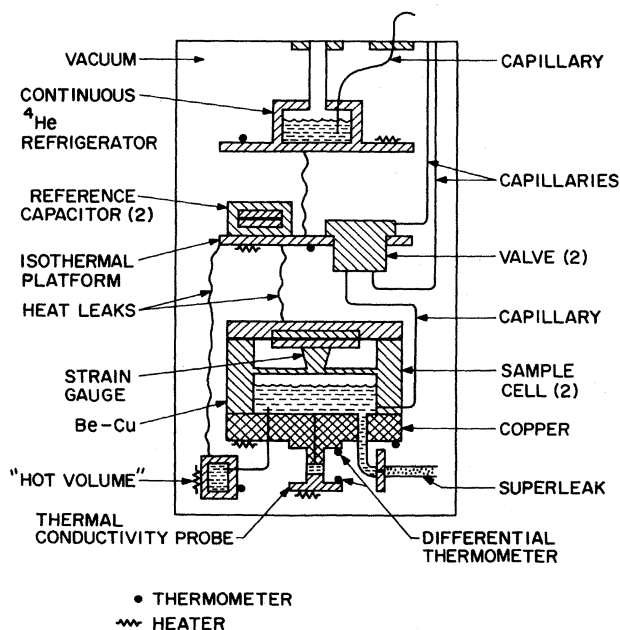


FIG. 1. Schematic diagram of the low-temperature portion of the apparatus. Only one sample cell, one valve, and one reference capacitor are shown.

in Fig. 1, through which the cells were filled. The reference capacitors for the pressure gauges (see Sec. IID) are also on this level. The "hot volume"<sup>25</sup> which was used to control the pressure in one of the cells was connected to this level through a heat leak of approximately  $4 \times 10^{-4}$  W/K. The mechanical supports and He II-filled capillaries connecting this stage to the refrigeration stage provided a heat leak of approximately  $3 \times 10^{-4}$  W. All wires coming from room temperature are thermally attached to the top flange of the vacuum can, to the refrigeration stage, and to the isothermal platform. The capillaries used to actuate the valves and those used to fill the cells are thermally attached to the top flange and the refrigeration stage.

The two sample cells were weakly thermally connected to the isothermal platform through the structural supports, whose heat leak was negligible, and through the 0.05-mm-i.d. filling capillaries, which provided a heat leak of  $3 \times 10^{-5}$  to  $2 \times 10^{-4}$  W, depending on the operating temperature of the cells.

The cells are similar to one described elsewhere,<sup>25</sup> the major differences being the locating of the low-temperature filling valve on the isothermal platform and the presence of the superleak connecting the cells. The top of the sample cell is the movable diaphragm of the pressure transducer (see Sec. IID below), which is a capacitive strain gauge of the type described by Straty and Adams.<sup>26</sup> Attached to the bottom of each cell is a small thermal conductivity probe<sup>23</sup> which was used to detect the  $\lambda$  point when calibrating the germanium thermometers and when making measurements close to  $T_\lambda$ . The cells are connected to the superleak by flanges with indium gaskets.

### B. Superleak

The superleak was made from a stainless-steel tube 4 cm long with an inner diameter of 0.37 cm and a wall thickness of 0.02 cm; for the present work, we used two different superleaks packed with nominally 0.3- and 0.05- $\mu\text{m}$ -diam alumina particles,<sup>27</sup> respectively. The packing was accomplished in the following manner: One end of the superleak was capped off and small amounts of alumina powder were alternately poured in the other end and tamped down with a steel rod inserted in the superleak. For the 0.05- and 0.3- $\mu\text{m}$  superleaks, the porosity was 0.68 and 0.69, respectively, and the flow impedance, measured at room temperature, was  $7 \times 10^{12}$  and  $2 \times 10^{12}$  cm<sup>-3</sup>, respectively.

### C. Thermometry

Carbon resistors were used with two leads as thermometers on the refrigeration stage and the hot volume, where accuracy was not essential. A carbon resistor on the isothermal stage was used in a five-wire ac resistance bridge similar to that shown in Fig. 4 of Ref. 25. Similar bridges were used with germanium thermometers<sup>28</sup> on the two sample cells. The main difference between these thermometer systems and similar arrangements in the past was the use here of 5-k $\Omega$  wire-wound resistors<sup>29</sup> rather than metal-film resistors or high-resistance wire as refer-

ences. This virtually eliminated the problem of thermometer drift as reported, for instance, by Steinberg and Ahlers.<sup>30</sup> Repeated measurements of the  $\lambda$ -point temperature at SVP indicate that the thermometer systems were stable to about  $30 \mu\text{K}$  over periods of several weeks at low temperatures and changed by no more than  $300 \mu\text{K}$  upon cycling between room temperature and 2 K.

The two germanium thermometers were each calibrated over the range  $1.6 \leq T \leq 2.172 \text{ K}$  against the sample vapor pressure on the 1958  $^4\text{He}$ -vapor-pressure scale ( $T^{58}$ ).<sup>31</sup> For this purpose we used the pressure gauge on one of the cells which had been calibrated previously against a (0–10 000)-Torr MKS Instruments Baratron gauge.<sup>32</sup> During this procedure the temperature was held constant to  $\pm 1 \mu\text{K}$  using the bridge and electronic regulation; the vapor pressure could then be measured with a resolution corresponding to about  $\pm 50 \mu\text{K}$ . Several checks on the calibration of the thermometers after cycling to room temperature demonstrated that it was not necessary to reestablish the temperature scale each time, allowing all measurements to be analyzed using the same parameters in the fitting equation. The bridge ratios  $\mathcal{R}$  and the corresponding temperatures during the calibration were fitted to the equation

$$\log_{10} \left[ \frac{T}{T_\lambda} \right] = \sum_{n=1}^3 A_n \left[ \log_{10} \left[ \frac{\mathcal{R}(1-\mathcal{R}_\lambda)}{\mathcal{R}_\lambda(1-\mathcal{R})} \right] \right]^n. \quad (2)$$

In order to establish  $T_\lambda$  as accurately as possible,  $\mathcal{R}_\lambda$  was determined during the calibration and at the time of the FP measurements with a resolution corresponding to  $\pm 1 \mu\text{K}$  using the thermal conductivity probe; within that resolution, our working temperature scale [Eq. (2)] will reproduce the fixed-point value  $T_\lambda = 2.172 000 \text{ K}$ . The deviations  $\delta T$  of  $T$  from that given by Eq. (2) have a root-mean-square value of about  $0.07 \text{ mK}$ , which is only slightly larger than our vapor-pressure resolution. They vary only slowly with  $T$  such that  $|d(\delta T)/dT| \leq 10^{-3}$  for all  $T$ . Therefore, the use of Eq. (2) in the data analysis without corrections for the temperature dependence of  $\delta T$  leads to errors of at most  $0.1\%$  in the FP. Our temperature scales for the two thermometers yielded  $1.763 34$  and  $1.763 30 \text{ K}$  for the upper  $\lambda$  point at the solidification curve, in excellent agreement with Kierstead's value of  $1.7633 \text{ K}$ .<sup>33</sup>

#### D. Pressure gauges

The top of each sample cell is an elastically deformable diaphragm made of beryllium-copper  $0.15 \text{ cm}$  thick and  $2.5 \text{ cm}$  in diameter (see Fig. 1). A slightly smaller copper plate is epoxied to a post in the center of the diaphragm; a second plate of the same size is fixed in position approximately  $80 \mu\text{m}$  from the first plate. The capacitor thus formed and a similar reference capacitor on the isothermal platform are used in conjunction with a ratio transformer<sup>34</sup> and a lock-in amplifier<sup>35</sup> in an ac bridge arrangement similar to that described in Ref. 25 (see also Fig. 2 of Ref. 30 or Fig. 2 of Ref. 36). The out-of-phase signal was minimized by adjusting a series resistance (typically a few ohms) in the appropriate lead from the pressure gauge or the reference capacitor. A resolution of 1

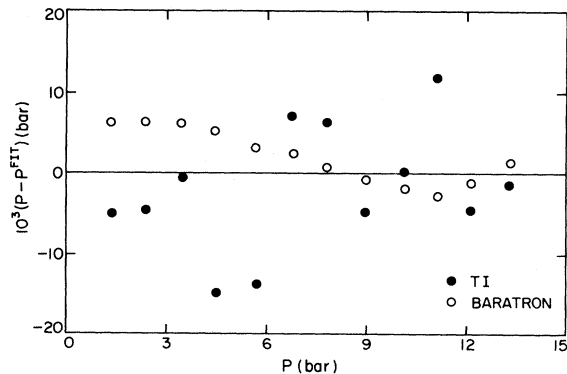


FIG. 2. Difference between the pressure measured with the TI and Baratron gauges and our fit to Eq. (3).

part in  $10^9$  in the capacitance was readily achieved and corresponds to a pressure resolution of  $3 \times 10^{-7} \text{ bar}$ .

The gauges were calibrated from 0–29 bar using a Texas Instruments (TI) quartz bourdon-tube gauge.<sup>37</sup> Because this gauge is not a primary pressure standard, several precautions were taken to minimize the possibility of systematic errors in our pressure scale. First, the TI gauge was returned to the company for a check on its calibration against their standard. We then used it and an MKS Instruments Baratron gauge<sup>32</sup> (which was also sent to its manufacturer for a calibration check) to calibrate the capacitive gauge on one of the cells over the range of the Baratron gauge (0–13 bar), and fitted these points to the equation<sup>38</sup>

$$P = A(1/\mathcal{R}_0 - 1/\mathcal{R}) + C(1/\mathcal{R}_0 - 1/\mathcal{R})^3, \quad (3)$$

where  $\mathcal{R}$  is the bridge ratio and  $A$ ,  $C$ , and  $\mathcal{R}_0$  are fitting parameters. The deviations from this fit for the Baratron and the TI gauge are plotted in Fig. 2 and show that there is good agreement between the two gauges. The deviation  $\delta P = P - P^{\text{FIT}}$  varies only slowly with pressure, so that  $|d(\delta P)/dP| < 2 \times 10^{-3}$  for all  $P$ . The final calibration points over the range 0–29 bar obtained using the TI gauge were also fitted to Eq. (3) with similar deviations occurring. Thus we expect that the use of this equation in the data analysis can lead to possible systematic errors of perhaps  $0.2\%$  in the FP. The pressure gauges on the cells had to be recalibrated after thermal cycles to room temperature. The parameter  $A$  in Eq. (3) changed typically by a few tenths of  $1\%$  upon cycling.

Figure 3 is a plot of the difference between our value of  $P_\lambda$  at a given  $T_\lambda$  and that of Kierstead<sup>33</sup> as a function of our measured  $P_\lambda$ . As mentioned in Sec. II C, the upper  $\lambda$ -point temperatures differ by less than  $10^{-4} \text{ K}$ ; the pressure difference at this temperature is indicated by an arrow. The deviations in Fig. 3 are well within the combined uncertainty in Kierstead's (0.05-atm) and our (0.04-bar) values.

#### E. Procedure

The FP was measured at vapor pressure in the following way. Helium was condensed in the cells until they were about  $80\%$  full, and the low-temperature valves were

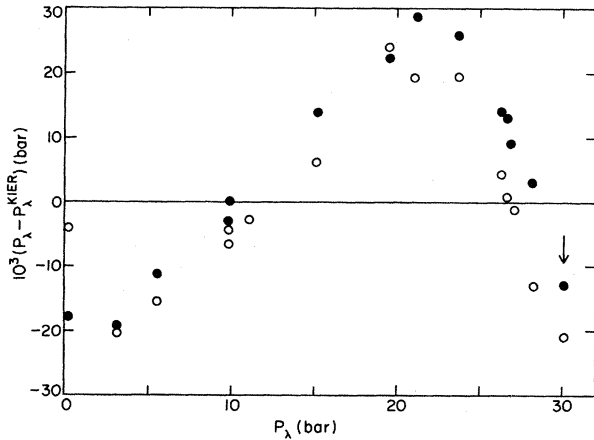


FIG. 3. Difference between our measured  $P_\lambda$  at a given  $T_\lambda$  and that of Kierstead (Ref. 37).

closed. Both cells were regulated at a fixed temperature with a stability of  $\pm 0.5 \mu\text{K}$  using the germanium thermometer bridge systems and electronic regulators.<sup>39</sup> The pressure in both cells remained constant at the vapor pressure. One of the cells was then raised from its initial temperature in intervals of about 0.3 mK for ten steps, the pressure being recorded initially and after each temperature increase. A typical plot of  $\Delta P/\Delta T$  vs  $\Delta T$ , in this case for  $T=2.1651$  K, is shown in Fig. 4. The variation of  $\Delta P/\Delta T$  with  $\Delta T$  is attributable to the variation of  $S(T)$  over the temperature interval  $\Delta T$ . Assuming the density  $\rho$  to be independent of  $T$ , we write Eq. (1) as

$$\Delta P = \int_{T_0}^{T_0 + \Delta T} \rho S dT = \rho S_0 \Delta T + \frac{\rho}{2} \left[ \frac{\partial S}{\partial T} \right]_{P_0} (\Delta T)^2 + \dots,$$

which gives for  $\Delta P/\Delta T$

$$\Delta P/\Delta T = \rho S_0 [1 + (C_0/2S_0 T_0) \Delta T] + \dots, \quad (4)$$

where the subscript indicates the temperature of the cooler cell and  $C$  is the specific heat of the liquid. In practice,  $S$  was determined by fitting the data to the equation

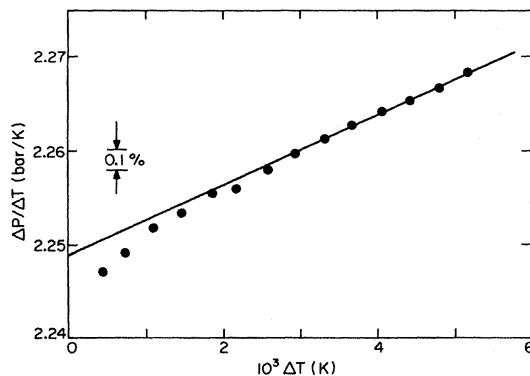


FIG. 4.  $\Delta P/\Delta T$  vs  $\Delta T$  for  $T=2.1651$  K at SVP. The line corresponds to a fit to Eq. (5) adjusting  $P_0$  and  $S_0$  and using the known value of the specific heat  $C_0$ .

$$P = P_0 + \rho S_0 \Delta T + (\rho C_0/2T_0)(\Delta T)^2 \quad (5)$$

with  $C_0$  fixed at its known value and  $S_0$  and  $P_0$  determined by the fitting program. The fit obtained in this way is indicated by the solid line in Fig. 4. The systematic deviations at small  $\Delta T$  are attributable to a very small constant additive error in  $\Delta T$  and have little influence on the value of  $S_0$  derived from the data. The standard errors of  $S_0$  given by the fits to the data were always less than a few parts in  $10^4$ .

Equation (1) and thus Eq. (5) are strictly applicable only for the case of a perfect superleak in which the normal fluid is truly at rest. Such a superleak is well approximated only by a porous medium made up of highly compacted, very small particles. In such a system the superfluid transition is severely suppressed. We used relatively open geometries (large particles) because we wanted to work near the *bulk* superfluid transition. In that case there is some normal fluid flow, compensated by superfluid flow, such that  $v_s \rho_s + v_n \rho_n = 0$  ( $v_s$  and  $v_n$  are the normal and superfluid velocities averaged over the width of the superleak); therefore, it was important to keep  $\Delta T$  sufficiently small throughout the measurements to avoid exceeding critical velocities in the counterflow. A plot of  $\Delta P/\Delta T$  vs  $\Delta T$  for  $T=2.1698$  K at SVP is shown in Fig. 5, where the line is again Eq. (5). The sudden decrease in  $\Delta P/\Delta T$  for  $\Delta T$  near 0.85 mK is due to the onset of dissipation at the critical velocity. In all measurements close to the  $\lambda$  point, only data obtained below the critical velocity were used to determine the entropy. At temperatures more than about 10 mK from  $T_\lambda$ , our  $\Delta T$ 's were never sufficiently large to observe the critical velocity (see Fig. 4, for example). At higher pressures a similar technique was used, with the modification that the pressure in the cooler cell was regulated to about  $\pm 5 \times 10^{-7}$  bar by controlling the temperature of the hot volume in a feedback loop similar to that shown in Fig. 1 of Ref. 25.

#### F. Errors

The possible error in  $S$  is the sum of several terms involving the resolution in the measurement of  $\Delta P$  and  $\Delta T$  and the uncertainty in the absolute temperature  $T$  and pressure  $P$ . The smallest  $\Delta P$  used was about 2 mbar with a resolution of the pressure gauge  $\delta(\Delta P)$  of  $10^{-3}$  mbar;

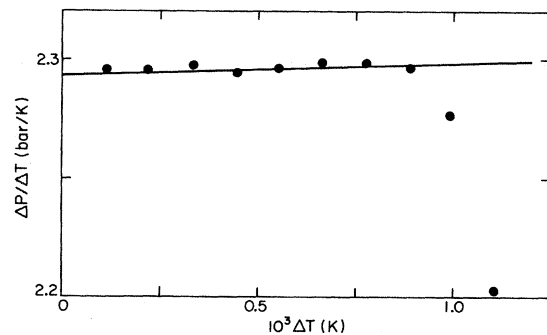


FIG. 5.  $\Delta P/\Delta T$  vs  $\Delta T$  for  $T=2.1698$  K at SVP showing the effect of the critical velocity. The line corresponds to Eq. (5) as in Fig. 4.

thus  $\delta(\Delta P)/\Delta P \approx 5 \times 10^{-4}$ . The temperature intervals  $\Delta T$  were usually 3 mK with a stability of about 1  $\mu$ K. The relative error is thus  $\delta(\Delta T)/\Delta T \approx 3 \times 10^{-4}$ . The uncertainty in the absolute pressure was at most about 0.04 bar. The resulting absolute error in  $S$  is negligible due to the relatively weak dependence of  $S$  on  $P$ . The absolute temperature depends upon the accuracy of the vapor-pressure measurements during the calibration of the thermometers. Our temperature scale was defined through Eq. (2) to reproduce the  $T^{58}$  vapor-pressure  $\lambda$ -point value of  $T_\lambda = 2.172\,000$  K (see Sec. II C above); we neglect here effects due to differences between  $T^{58}$  and the thermodynamic scale. For  $T < T_\lambda$  our temperature scale is believed to be accurate to  $\pm 0.1\%$  of  $T_\lambda - T$ . This corresponds to a possible relative error in  $S$  of

$$\frac{\delta S}{S} = \left| \frac{1}{S} \frac{\partial S}{\partial T} \right| \delta T \approx 10^{-3}$$

at the lowest temperatures; the error approaches zero as  $\delta T$  approaches zero near  $T_\lambda$ .

The relative error in  $\Delta T$  due to systematic deviations from Eq. (2) is no more than  $1 \times 10^{-3}$ . The relative error in  $\Delta P$  due to systematic deviations from Eq. (3) could be somewhat larger, and we therefore investigated the effect of adding additional terms to that equation. Adding a quadratic term yielded coefficients for the quadratic and the cubic terms with standard errors roughly equal to their value. This implies that one or the other of them (but, of course, not both) may be omitted without causing statistically significant deviations. In order to determine the effect on the entropy of the particular form of the fitting equation for the pressure, we computed values of  $S$  using Eq. (3) ( $S_3$ ), as well as values based on a fitting equation with a quadratic and a cubic term ( $S_{2,3}$ ). The relative difference  $(S_{2,3} - S_3)/S_3$  is shown in Fig. 6 as a function of  $P$ . We see that the detailed form of the equation can change  $S$  by 0.2 to 0.3% and regard this as an estimate of possible systematic errors from uncertainties in our pressure scale.

We conclude that the total random errors in  $S$  are no more than 0.1% over most of the temperature range. Within about 20 mK of  $T_\lambda$  they become slightly larger

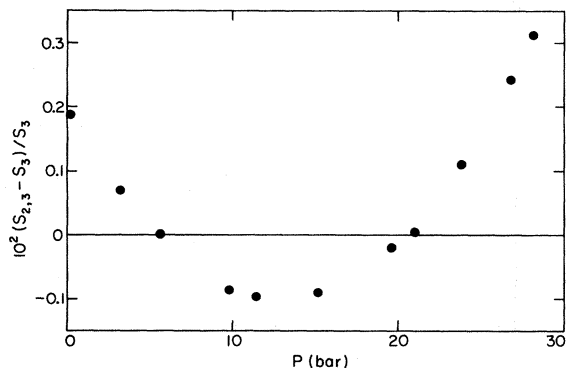


FIG. 6. Relative difference between values of  $S$  obtained using Eq. (3) ( $S_3$ ) and using Eq. (3) plus a quadratic term ( $S_{2,3}$ ) for the pressure scale.

because of the reduced sizes of the intervals  $\Delta P$  and  $\Delta T$ . The total (possibly pressure-dependent) systematic errors in  $S$  are no more than 0.4%.

### III. RESULTS

All of our measured values of the entropy per unit volume at different pressures and temperatures for the 0.3- $\mu$ m powder are given in Table I and for the 0.05- $\mu$ m powder at SVP in Table II. Those values are based on a pressure scale represented by Eq. (3). Near  $T_\lambda$   $S(T)$  varies extremely rapidly with  $T$ ; the error  $(\partial S / \partial T)_P \delta T$  in  $S$  due to the uncertainty  $\delta T$  in  $T$  will thus become significant even if  $T$  is measured to the relatively high accuracy of, e.g.,  $10^{-4}$  K on the accepted temperature scale. For that reason we were particularly careful in this work to locate  $T_\lambda(P)$  on our working temperature scale with the very high resolution of 2  $\mu$ K and to measure the distance  $t = 1 - T/T_\lambda(P)$  from  $T_\lambda$  along an isobar with an accuracy equal to the larger of  $10^{-6}$  or 0.1% of  $t$ . We therefore quote  $t$  as well as  $T$  in the tabulation of our data.

To facilitate the comparison of our results to those of other authors, we fit the entropy per mol derived from our measurements along the vapor-pressure curve, along the  $\lambda$  line, and along several isotherms to simple empirical functions. For temperatures within 20 mK of  $T_\lambda$ , the molar volume used to convert the entropy per unit volume to entropy per mol was determined from the  $\lambda$ -line values of the density from Kierstead<sup>33</sup> and the thermal-expansion coefficient data of Mueller *et al.*<sup>25</sup> For lower temperatures we used Maynard's<sup>16</sup> values for the density.

The FP measurements at vapor pressure were done twice with different size powders in the superleak (0.05 and 0.3  $\mu$ m). A simultaneous fit of both sets of data to the equation

$$S_{\text{SVP}} = At^x + Bt^2 + Ct + D \quad (6)$$

yielded

$$A = 52.960,$$

$$B = -0.955,$$

$$C = -53.436,$$

$$D = 6.301,$$

and

$$x = 1.328,$$

where  $t = (2.172 - T)/2.172$  and where  $S_{\text{SVP}}$  is in  $\text{J mol}^{-1} \text{K}^{-1}$ . Deviations from the fit for the two powders are shown in Fig. 7. The agreement demonstrates that there is no significant effect of the size of the powder on the FP for the range of temperatures in which we were working. All of the measurements under pressure were taken with the 0.3- $\mu$ m powder in the superleak.

In Fig. 8 we compare the above fit to the vapor-pressure entropy from 1.6 to 2.15 K to the results of several authors. There is excellent agreement with the recent data of Hoffer and Phillips.<sup>19</sup> The agreement is particularly satisfying since the entropies of Hoffer and Phil-

TABLE I. Entropy per unit volume  $\rho S$  at various pressures  $P$  and temperatures  $T$  for the 0.3- $\mu\text{m}$  powder superleak. Also given is the reduced temperature  $t = 1 - T/T_\lambda(P)$ .

$P$ (bar)	$T$ (K)	$t$	$\rho S$ ( $\text{J cm}^{-3} \text{K}^{-1}$ )
SVP	2.1705	0.000 690 6	0.2299
SVP	2.1703	0.000 790 1	0.2296
SVP	2.1698	0.001 013	0.2294
SVP	2.1681	0.001 794	0.2275
SVP	2.1651	0.003 177	0.2250
SVP	2.1597	0.005 662	0.2208
SVP	2.1501	0.010 07	0.2145
SVP	2.0995	0.033 38	0.1854
SVP	1.9988	0.079 73	0.1407
SVP	1.8980	0.126 14	0.1062
SVP	1.7970	0.172 65	0.07920
SVP	1.6955	0.219 37	0.05778
SVP	1.5934	0.266 39	0.04083
3.17	2.1297	0.005 608	0.2199
3.17	2.1204	0.009 939	0.2139
3.17	2.1034	0.017 89	0.2031
3.17	2.0730	0.031 72	0.1861
3.27	2.0001	0.065 65	0.1531
3.50	1.8982	0.112 27	0.1155
3.55	1.7986	0.158 61	0.08536
4.65	1.6979	0.201 32	0.06529
5.64	2.1082	0.003 164	0.2238
5.64	2.1030	0.005 640	0.2194
5.64	2.0944	0.009 70	0.2134
5.64	2.0730	0.019 82	0.1996
5.88	1.9990	0.053 58	0.1631
6.43	1.7972	0.146 65	0.09389
6.91	1.8982	0.096 42	0.1260
9.22	1.6984	0.180 66	0.07344
9.86	2.0585	0.003 161	0.2209
9.87	2.0540	0.005 330	0.2178
9.87	2.0444	0.010 01	0.2109
10.05	1.9990	0.030 89	0.1847
10.52	1.8992	0.077 20	0.1396
10.97	1.7972	0.124 13	0.1054
11.53	2.0422	0.000 975 0	0.2241
11.53	2.0377	0.003 147	0.2199
11.53	2.0328	0.005 582	0.2160
11.53	2.0279	0.007 981	0.2126
12.20	1.9138	0.060 02	0.1540
12.40	1.7970	0.116 12	0.1093
15.24	1.6970	0.149 56	0.08724
15.27	1.9895	0.002 766	0.2176
15.27	1.9829	0.006 120	0.2127
15.27	1.9751	0.010 01	0.2072
15.27	1.9605	0.017 33	0.1973
15.27	1.8982	0.048 53	0.1628
15.27	1.7970	0.099 28	0.1196
16.50	1.7970	0.091 44	0.1246
17.60	1.8982	0.032 69	0.1770
18.18	1.7970	0.080 55	0.1318
19.79	1.9294	0.000 992	0.2185
19.79	1.9251	0.003 175	0.2127
19.79	1.9204	0.005 646	0.2090
19.79	1.9165	0.007 633	0.2060
19.79	1.9144	0.008 750	0.2043
19.79	1.7970	0.069 53	0.1392
20.03	1.6970	0.119 64	0.1015
21.11	1.9044	0.003 747	0.2102

TABLE I. (Continued.)

$P$ (bars)	$T$ (K)	$t$	$\rho S$ ( $\text{J cm}^{-3} \text{K}^{-1}$ )
21.11	1.8980	0.007 074	0.2052
21.37	1.7970	0.057 97	0.1475
23.60	1.7980	0.040 16	0.1621
23.79	1.8597	0.005 688	0.2041
23.79	1.8561	0.007 601	0.2014
23.84	1.8531	0.008 836	0.1993
25.10	1.6970	0.082 35	0.1222
25.17	1.7980	0.020 74	0.1742
26.91	1.8162	0.001 797	0.2065
26.91	1.8136	0.003 200	0.2040
26.91	1.8091	0.005 684	0.1998
26.91	1.8051	0.007 852	0.1970
27.26	1.7980	0.008 617	0.1949
27.38	1.7588	0.028 99	0.1685
28.14	1.7894	0.005 070	0.1989
28.14	1.7847	0.007 652	0.1946
28.61	1.7588	0.017 73	0.1801
28.65	1.6970	0.051 81	0.1425

lips are calorimetric values and thus subject to temperature-scale errors quite different from those of FP measurements. There is also good agreement, particularly at the higher temperatures, with the FP measurements of van den Meijdenberg *et al.*<sup>10</sup> However, the values at 0 bar of Sudraud and Varoquaux<sup>11</sup> differ systematically from ours by 1–2 % more than the combined error estimates of 1.5%. At 24 bar, where comparison is possible at 1.7 and 1.8 K, their measurements are about 2% less than ours. The systematic deviation from Maynard's<sup>16</sup> values are probably caused in part by his fitting procedure (see Sec. I). All measurements except those of Maynard and Sudraud and Varoquaux are within the respective author's and our combined error estimates.

We determined the entropy  $S_\lambda$  along the  $\lambda$  line by adding the small quantity

$$\Delta S = \int_{T_0}^{T_\lambda} (C_p/T) dT \quad (7)$$

TABLE II. Entropy per unit volume  $\rho S$  at SVP for various temperatures for the 0.05- $\mu\text{m}$  powder superleak.

$T$ (K)	$t$	$\rho S$ ( $\text{J cm}^{-3} \text{K}^{-1}$ )
1.6000	0.263 36	0.042 12
1.6500	0.240 32	0.049 75
1.7000	0.217 32	0.058 60
1.7501	0.194 26	0.068 66
1.8000	0.171 27	0.079 98
1.8500	0.148 25	0.092 79
1.9000	0.125 23	0.1070
1.9500	0.102 21	0.1233
2.0000	0.079 20	0.1414
2.0500	0.056 18	0.1622
2.1000	0.033 15	0.1860
2.1500	0.010 14	0.2143
2.1597	0.005 645	0.2210

to our measurements of the entropy at several reduced temperatures  $t$  along an isobar, where  $t \lesssim 10^{-2}$ . This procedure is the inverse of the one used by Greywall and Ahlers<sup>15</sup> to obtain  $S(T)$  from  $S_\lambda$ . We used the heat-capacity function (measured in  $\text{J mol}^{-1} \text{K}^{-1}$ ) (Ref. 5)

$$C_p = (-A \ln t + B + Dt \ln t + Et)$$

with

$$A = 5.102 - 0.056 52 P_\lambda + 9.643 \times 10^{-4} P_\lambda^2,$$

$$B = 15.57 - 0.3601 P_\lambda + 4.505 \times 10^{-3} P_\lambda^2,$$

$$D = 14.5 - 6.119 P_\lambda,$$

and

$$E = -69.0 - 19.08 P_\lambda,$$

where  $P$  is in bar; however, the result is not sensitive to the exact functional form of  $C_p$  because  $S_\lambda - S$  is small. The  $S_\lambda$ 's obtained in this way are given in Table III for various pressures and reduced temperatures. We note that

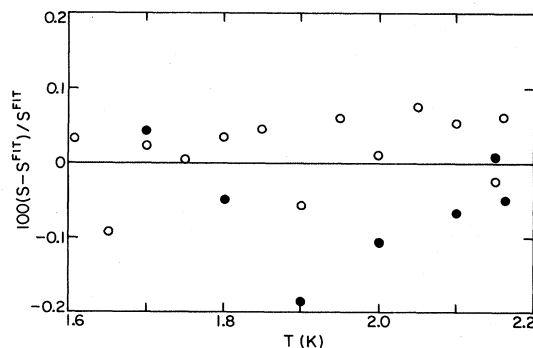


FIG. 7. Deviations in percent of our measured entropy at SVP from that given by Eq. (6) for the two superleaks. Closed circles: 0.3  $\mu\text{m}$ . Open circles: 0.05  $\mu\text{m}$ .

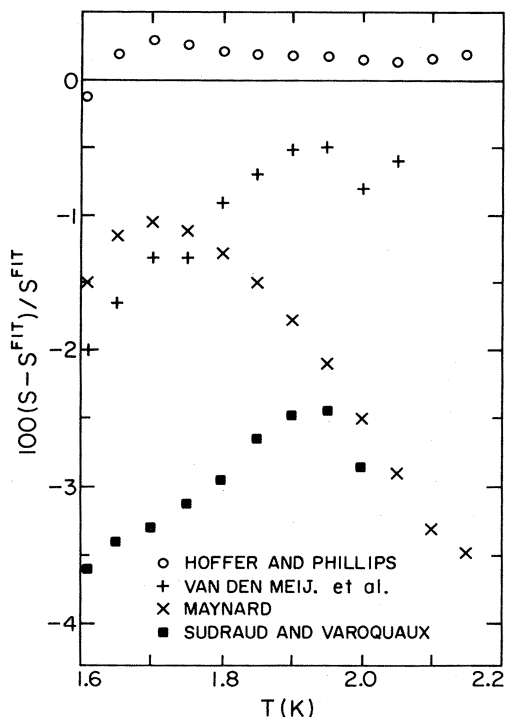


FIG. 8.  $S$  at SVP as determined by several authors compared to Eq. (6).

$S_\lambda$  does not depend systematically or significantly upon the value of  $t$  at which  $S(T)$  was measured. The averages of the  $S_\lambda$  values at a given pressure were fit to the empirical equation<sup>14</sup>

$$S_\lambda = At_\phi^x + Bt_\phi + C \quad (8)$$

and yielded

$$A = 12.350 ,$$

$$B = -5.27 ,$$

$$x = -0.0264 ,$$

$$T_\phi = 2.215 ,$$

$$C = -7.275 ,$$

$$t_\phi = (T_\phi - T_\lambda) / T_\phi .$$

Here  $S_\lambda$  is in  $\text{J mol}^{-1} \text{K}^{-1}$ . Figure 9 shows the deviations from Eq. (8) of our measurements, of Lounasmaa's calorimetric entropies,<sup>13</sup> and of Eq. (8) with the coefficients determined by Ahlers.<sup>14</sup> [Note that Eq. (8) with Ahlers's coefficients was also used by Maynard<sup>16</sup> to determine  $S_\lambda$  for his fits along isobars.] The agreement of all the data is well within the systematic errors anticipated by the original authors.

TABLE II. Entropy per mol close to  $T_\lambda$  and the derived  $S_\lambda$  at various pressures.

$P$ (bar)	$t$	$S$ ( $\text{J mol}^{-1} \text{K}^{-1}$ )	$S_\lambda$ ( $\text{J mol}^{-1} \text{K}^{-1}$ )
SVP	0.001 794	6.236	6.331
SVP	0.003 177	6.164	6.322
SVP	0.005 662	6.050	6.315
SVP	0.010 07	5.881	6.320
3.17	0.005 608	5.800	6.051
3.17	0.009 939	5.642	6.058
5.64	0.003 164	5.754	5.900
5.64	0.005 640	5.646	5.890
5.64	0.009 70	5.492	5.886
9.87	0.003 161	5.486	5.624
9.87	0.005 330	5.409	5.630
9.87	0.010 01	5.242	5.627
11.53	0.003 147	5.396	5.531
11.53	0.005 582	5.303	5.530
11.53	0.007 981	5.220	5.530
15.27	0.002 766	5.210	5.327
15.27	0.006 120	5.096	5.333
15.27	0.010 01	4.968	5.334
19.79	0.003 175	4.964	5.092
19.79	0.005 646	4.879	5.092
19.79	0.007 633	4.812	5.090
19.79	0.008 750	4.772	5.086
21.11	0.003 747	4.870	5.016
21.11	0.007 074	4.757	5.015
23.79	0.005 688	4.669	4.878
23.79	0.007 601	4.608	4.879
26.91	0.003 200	4.596	4.720
26.91	0.005 684	4.505	4.712
26.91	0.007 852	4.440	4.717
27.26	0.008 617	4.389	4.689
28.14	0.005 070	4.458	4.644
28.14	0.007 652	4.368	4.637



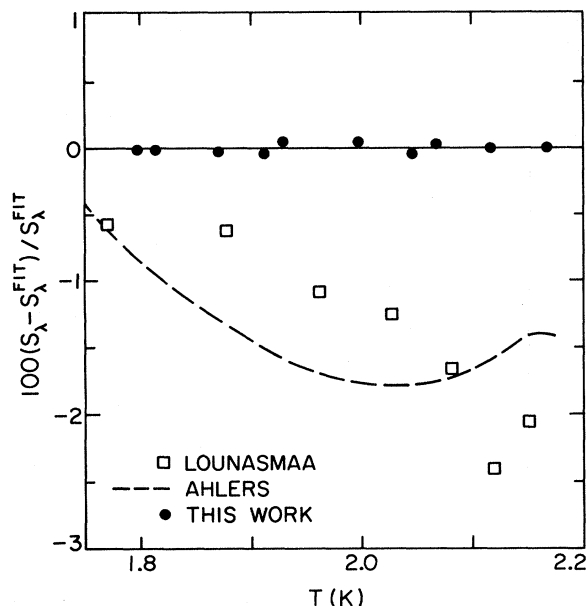


FIG. 9. Deviations from Eq. (8) of our  $\lambda$ -point entropies, Lounasmaa's values derived from specific-heat measurements (Ref. 13), and Eq. (8) using the coefficients determined by Ahlers (Ref. 14).

In addition to the measurements of the specific heat by Ahlers,<sup>14</sup>  $C_p$  can also be obtained from the thermal-expansion ( $\beta_p$ ) measurements of Mueller *et al.* [see Sec. VD of Ref. 25, especially Eq. (5.5)]. We therefore also used  $C_p$  obtained from  $\beta_p$  to determine  $\Delta S$  from Eq. (7). For reduced temperatures less than 0.003, the resulting  $S_\lambda(\beta_p)$  differed from Eq. (8) by less than 0.1% for all pressures.

Equation (8) can be used to compute the derivative  $(dS/dT)_\lambda$  of the entropy at  $T_\lambda$ . That result can be compared with independent measurements of other thermodynamic parameters. At SVP,  $(dS/dT)_\lambda$  was deduced<sup>40</sup> from the thermal-expansion measurements of Van De Grift.<sup>41</sup> At higher pressures, values were obtained from simultaneous measurements of  $C_v$  and  $(\partial P/\partial T)_v$ .<sup>14</sup> In Table IV the data are collected and compared with Eq. (8). The agreement is very good for pressures up to about 15 bar. For higher pressures there are significant differ-

TABLE IV. Values of  $(dS/dT)_\lambda$  obtained from measurements of other thermodynamic parameters and from Eq. (8).

$P_\lambda$ (bar)	$T_\lambda$ (K)	$(dS/dT)_\lambda$ ( $\text{J mol}^{-1} \text{K}^{-2}$ )	
		Eq. (8)	Other
0.05	2.172	10.9	10.9 <sup>a</sup>
1.65	2.157	8.6	8.6 <sup>b</sup>
7.33	2.095	5.3	5.5 <sup>b</sup>
15.03	1.998	4.0	3.8 <sup>b</sup>
18.18	1.954	3.7	3.4 <sup>b</sup>
22.53	1.889	3.4	3.2 <sup>b</sup>
25.87	1.836	3.3	2.9 <sup>b</sup>

<sup>a</sup>References 40 and 41.

<sup>b</sup>Reference 14.

TABLE V. Parameters obtained from fitting the data along isotherms to Eq. (9) for several temperatures. In Eq. (9) the units of  $P$  are bar and those of  $S$  are  $\text{J mol}^{-1} \text{K}^{-1}$ .

	$10^8 A$	$10^3 B$	$10^2 C$	$D$	$x$
1.7 K	0.0014	1.1295	1.652	1.613	7.0
1.8 K	5.0	0.8532	3.086	2.200	5.0
1.9 K	0.2665	2.310	2.782	2.940	6.0
2.0 K	5.6916	2.3707	4.320	3.878	6.0

ences which, we believe, are attributable to small systematic errors in the  $C_v$  and  $(\partial P/\partial T)_v$  measurements.<sup>14</sup>

The data along an isotherm were fitted to equations of the form

$$S = AP^x + BP^2 + CP + D, \quad (9)$$

where  $P$  is the pressure. The values of the parameters for several isotherms are given in Table V. In Fig. 10 we

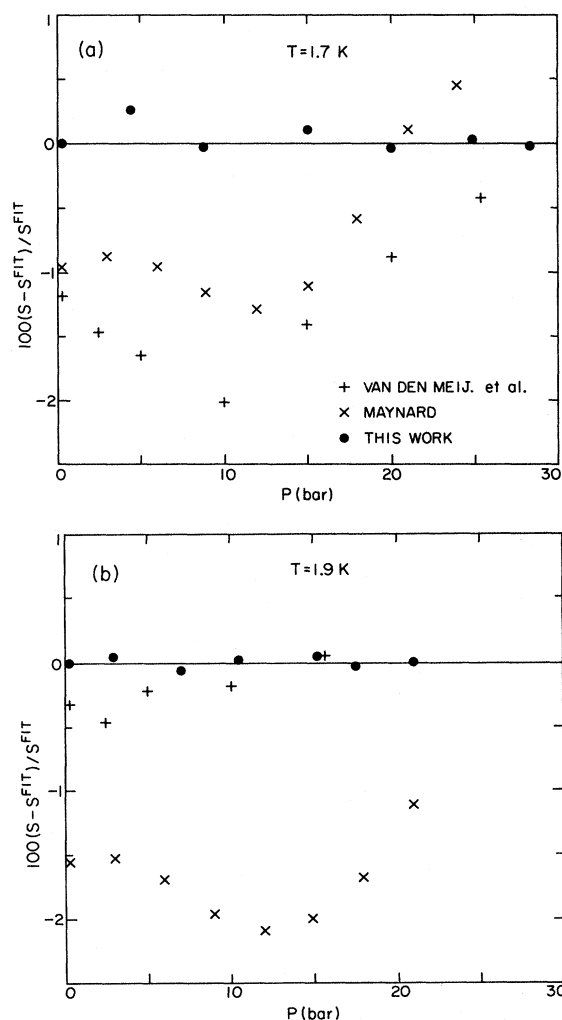


FIG. 10. Deviations in percent of our measured values and those of Maynard (Ref. 16) and van den Meijdenberg *et al.* (Ref. 10) from Eq. (9) using the parameters in Table V for (a) the 1.7-K isotherm and (b) the 1.9-K isotherm.

show the deviations of data by Maynard<sup>15</sup> and van den Meijdenberg *et al.*<sup>10</sup> (vdM) from our fits along the 1.7- and 1.9-K isotherms. Note that both in Fig. 10 and in the comparison at SVP (Fig. 8) the agreement with vdM improves as one nears  $T_\lambda$ , which suggests that the differences in  $S$  are the result of differences in the temperature scales that become less as  $T_\lambda$  is approached. The comparison with Maynard shows a somewhat less regular but similar behavior for the two isotherms shown.

#### IV. SUMMARY

We measured the FP of He II from 1.6 K to near  $T_\lambda$  for pressures from SVP to 29 bar with an overall accuracy of 0.5%. We used these results and the known specific heat near  $T_\lambda(P)$  to obtain the entropy  $S_\lambda(P)$  along the  $\lambda$  line. At SVP the measurements were made with 0.05- and 0.3- $\mu\text{m}$  powders in the superleak. The two sets of data agree within about 0.2%. All measurements under pres-

sure were done with the 0.3- $\mu\text{m}$  powder. The entropy per mol derived from these results agrees with recent unpublished calorimetric values by Hoffer and Phillips at vapor pressure to within 0.3%. The agreement with other FP measurements and the entropy derived from sound measurements was not as good but, in most cases, was within the combined error estimates.

The entropy per unit mass obtained from our data will be used<sup>20</sup> to determine with increased accuracy the superfluid fraction  $\rho_s/\rho$  from second-sound velocity measurements<sup>15</sup> according to the relation  $u_2^2 = S^2 T \rho_s / \rho_n C_p$  where  $C_p$  is the specific heat at constant pressure.

#### ACKNOWLEDGMENTS

We are grateful to J. K. Hoffer and N. E. Phillips for providing us with their unpublished results. This work was supported by National Science Foundation Grant No. DMR-79-23289.

- <sup>1</sup>G. Ahlers, in *Quantum Liquids*, edited by J. Ruvalds and T. Regge (North-Holland, Amsterdam, 1978), p. 1; *Rev. Mod. Phys.* **52**, 49 (1980).
- <sup>2</sup>K. G. Wilson, *Phys. Rev. B* **4**, 3174, 3184 (1971). For a review of the application to critical phenomena, see K. G. Wilson and J. Kogut, *Phys. Rep.* **12C**, 76 (1974), or M. E. Fisher, *Rev. Mod. Phys.* **46**, 597 (1974).
- <sup>3</sup>L. D. Landau, *J. Phys. (Moscow)* **5**, 71 (1941).
- <sup>4</sup>I. M. Khalatnikov, *Introduction to the Theory of Superfluidity* (Benjamin, New York, 1965).
- <sup>5</sup>For a review of the properties of <sup>4</sup>He near the  $\lambda$  line, see G. Ahlers, in *The Physics of Liquid and Solid Helium*, edited by K. H. Bennemann and J. B. Ketterson (Wiley, New York, 1976), Vol. 1, Chap. 2.
- <sup>6</sup>H. London, *Proc. R. Soc. London, Ser. A* **171**, 484 (1939).
- <sup>7</sup>J. F. Allen and H. Jones, *Nature* **141**, 243 (1938).
- <sup>8</sup>L. Meyer and J. H. Mellink, *Physica (Utrecht)* **13**, 197 (1947).
- <sup>9</sup>D. F. Brewer and D. O. Edwards, *Proc. Phys. Soc. London, Sect. A* **71**, 117 (1958).
- <sup>10</sup>C. J. N. van den Meijdenberg, K. W. Taconis, and R. de Bruyn Ouboter, *Physica (Utrecht)* **27**, 197 (1961).
- <sup>11</sup>M. Sudraud and E. J. Varoquaux, *Physica* **94B**, 303 (1978).
- <sup>12</sup>R. W. Hill and O. V. Lounasmaa, *Philos. Mag.* **2**, 143 (1957).
- <sup>13</sup>O. V. Lounasmaa, *Cryogenics* **1**, 1 (1961).
- <sup>14</sup>G. Ahlers, *Phys. Rev. A* **8**, 530 (1973).
- <sup>15</sup>D. S. Greywall and G. Ahlers, *Phys. Rev. A* **1**, 2145 (1973).
- <sup>16</sup>J. Maynard, *Phys. Rev. B* **14**, 3868 (1976).
- <sup>17</sup>See Ref. 28 of J. Maynard, *Phys. Rev. B* **14**, 3868 (1976).
- <sup>18</sup>J. Heiserman, J. P. Hulin, J. Maynard, and I. Rudnick, *Phys. Rev. B* **14**, 3862 (1976).
- <sup>19</sup>J. K. Hoffer and N. E. Phillips (private communication).
- <sup>20</sup>A. Singaas and G. Ahlers (unpublished).
- <sup>21</sup>Many of the features of the apparatus are similar to that described in Ref. 25 and references therein.
- <sup>22</sup>L. D. DeLong, O. G. Symko, and J. C. Wheatley, *Rev. Sci. Instrum.* **42**, 147 (1971).
- <sup>23</sup>G. Ahlers, *Phys. Rev. A* **3**, 696 (1971).
- <sup>24</sup>P. R. Roach, J. B. Ketterson, and M. Kuchnir, *Rev. Sci. Instrum.* **43**, 898 (1972).
- <sup>25</sup>K. H. Mueller, G. Ahlers, and F. Pobell, *Phys. Rev. B* **14**, 2096 (1976).
- <sup>26</sup>G. C. Straty and E. G. Adams, *Rev. Sci. Instrum.* **40**, 1939 (1969).
- <sup>27</sup>Union Carbide Corporation, Linde alumina polishing powder, 0.3 and 0.05  $\mu\text{m}$ .
- <sup>28</sup>Cryocal, Model No. CR 1000 <sup>3</sup>He.
- <sup>29</sup>General Resistance, 5 k $\Omega$  ( $\pm 0.01\%$ ), 8E16A.
- <sup>30</sup>V. Steinberg and G. Ahlers, *J. Low Temp. Phys.* **53**, 255 (1983).
- <sup>31</sup>H. van Dijk, M. Durieux, J. R. Clement, and J. K. Logan, *The 1958 <sup>4</sup>He scale of Temperatures*, Natl. Bur. Stand. (U.S.) Monograph No. 10 (U.S. GPO, Washington, D.C., 1960).
- <sup>32</sup>MKS Instruments, Inc., type BHS-1000 Baratron pressure gauge.
- <sup>33</sup>H. A. Kierstead, *Phys. Rev.* **162**, 153 (1967).
- <sup>34</sup>Singer, ac Ratio Standard Model No. 1011.
- <sup>35</sup>Princeton Applied Research, Model No. 124A with Model No. 185 preamplifier.
- <sup>36</sup>M. Chan, M. Ryschkewitsch, and H. Meyer, *J. Low Temp. Phys.* **26**, 213 (1977).
- <sup>37</sup>Texas Instruments, Inc., Precision pressure gauge, Model No. 145-02.
- <sup>38</sup>D. S. Greywall and P. A. Busch, *Rev. Sci. Instrum.* **51**, 509 (1980).
- <sup>39</sup>Linear Research, San Diego, California, Model No. LR-130 temperature controller.
- <sup>40</sup>*The Physics of Liquid and Solid Helium*, Ref. 5; see the reference on p. 99.
- <sup>41</sup>C. T. Van De Grift, Ph.D. thesis, University of California, Irvine, California, 1974.